Journal of Theoretical and Applied Information Technology
30th April 2012. Vol. 38 No.2

ISSN: 1992-8645 www.jatit.org E-ISSN: 1817-3195

A NOVEL DESIGN OF QUARTER WAVE-SHIFTED DISTRIBUTED FEEDBACK SEMICONDUCTOR LASER FOR HIGH-POWER SINGLE-MODE OPERATION

[1]A. MOUMEN, [2]A. ZATNI, [3]A. ELKAAOUACHI, [4]H. BOUSSETA, [5]A. ELYAMANI.

[1,4,5]PhD Student, M.S.I.T Laboratory, Department of Computer Engineering high school of technology, Ibn Zohr University Agadir Morocco.

[2]Prof., Department of Computer Engineering, high school of technology, Agadir Morocco

[3]Prof., Department of physics, faculty of sciences, Ibn Zohr university Agadir Morocco

E-mail: [1]abdelkarim.moumen@gmail.com

ABSTRACT

The spatial hole burning effect has been known to limit the performance of distributed feedback semiconductor diode lasers. As the biasing current of a single quarterly-wavelength-shifted distributed feedback diode laser increase, the gain margin reduces. Therefore, the maximum single-mode output power of the quarterly-wavelength-shifted distributed feedback diode laser is restricted to a relatively low power operation. The spatial hole burning phenomenon caused by the intense electric field leads to a local carrier depletion at the centre of the cavity. Such a change in carrier distribution alters the refractive index along the laser cavity an ultimately affects the lasing characteristics. In order to ensure a large gain margin ($\Delta\alpha L$) between the lasing mode and the most probable side, and also a uniform internal field distribution, subsequently a stable single longitudinal mode operation, distributed feedback lasers structures with modifications in the corrugation will be considered. Namely, the inclusion of phase-shifts and non-uniform coupling coefficients is presented with a comparative analysis of the laser performances in the above-threshold regime

Keywords: *Distributed feedback laser (DFB), distributed coupling coefficient (DCC), phase shift (PS), transfer matrix method (TMM),*

1. INTRODUCTION

In the last decade, both coherent optical communication systems (COCS) and wavelength division multiplexing (WDM) have received worldwide attention. It is important that the semiconductor diodes lasers used in these systems demonstrate a stable single mode with low threshold, high output optical power and reduced spatial hole burning (SHB) [1], distributed feedback (DFB) semiconductor laser diode is one of the favourite candidates as an optical source. The conventional DFB laser was first proposed and analysed [1]-[2]-[3] the main disadvantage of this laser was the mode degeneracy and a high threshold. A phase shift along laser cavity can be introduced to remove the mode degeneracy and decrease the threshold. Numerical simulations have shown that lowest threshold can be achieved if the phase shift is located at the centre of the laser cavity and its value is fixed at 90^0 [7]. This laser is known as a quarter-wavelength-shift (QWS) DFB laser. However, presence of the phase shift in the grating of DFB laser generally causes spatial no-uniformity of photon and carrier densities along the cavity [1]-[13]. This phenomenon, called spatial hole burning (SHB) effect, reduces the performances of QWS especially for large coupling coefficient length product ($\kappa L > 1.75$) and at high injection currents [7].However a high κL DFB laser is more attractive due to low threshold current density, large amplitude modulation, small line-width power product, as well as low reflection sensitivity. Several designs have been proposed to reduce the SHB effect. For example the multi-phase shifts (MPS DFB) placed along the laser cavity [18], the corrugation-pitch-modulated (CPM DFB) [9], and distributed coupling coefficient (DCC DFB) along the laser cavity [1]- [4]. We have already introduced quarter-wavelength-shift distributed feedback laser with a Gaussian profile of the

Journal of Theoretical and Applied Information Technology
30th April 2012. Vol. 38 No.2

ISSN: 1992-8645 www.jatit.org E-ISSN: 1817-3195

coupling coefficient (GPCC QWS DFB) structure which has good stability against SHB effect.

This paper aims at to show that this novel laser structure may strongly improve the laser performance above threshold, by maintaining uniform internal field profile along the cavity so reducing the strong hole burning, when compared with currently quarter wavelength shift structures.

The paper is organized as follows: Section II is devoted to introduce the model and theory of analysis in the frame of transfer matrix method. In section III the numerical results of structures lasers under study are presented. Finally, the main conclusions are summarized in section IV.

2. MODEL DESCRIPTION

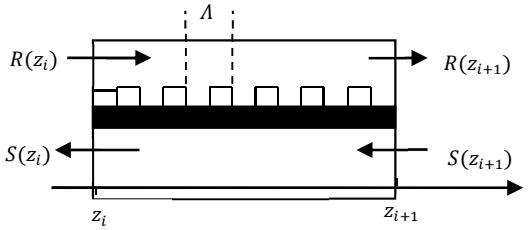

Fig. 1. A simplified schematic diagram for a one dimensional corrugated DFB laser diode section

The model has been used in the present work describes the laser cavity by a finite number of subsections (M sections) (Fig. 1) each one defined by complex matrix relating two counter-running waves due to the coupled wave mode equation. In each subsection all the parameters are kept constant, also the reflectivity at the end facets supposed to be zero. The analysis followed in this work called transfer matrix method (TMM). Where the whole matrix that describes the field propagation inside the laser cavity is (T) and it is $2x2$ complex matrix, which is the product of successive matrices related to each subsection.

$$\boldsymbol{T} = \begin{bmatrix} \boldsymbol{t_{11}} & \boldsymbol{t_{11}} \\ \boldsymbol{t_{11}} & \boldsymbol{t_{11}} \end{bmatrix} = \prod_{i=1}^{M} \begin{bmatrix} \boldsymbol{t_{11}(z_i)} & \boldsymbol{t_{11}(z_i)} \\ \boldsymbol{t_{11}(z_i)} & \boldsymbol{t_{11}(z_i)} \end{bmatrix} \quad (1)$$

Where $z_i = i\frac{L}{M} = i\Delta z$, L and M are the cavity length and total number of subsections, and $t_{jk}(j,k = 1,2)$ are given respectively by [5]:

$$\boldsymbol{t_{11}(z_i)} = \frac{[E^+(z_i) - \rho(z_i)^2 E^-(z_i)]}{1-\rho(z_i)^2} \quad (2)$$

$$\boldsymbol{t_{12}(z_i)} = \frac{-\rho(z_i)[E^+(z_i) - E^-(z_i)]}{1-\rho(z_i)^2} e^{-j\Omega} \quad (3)$$

$$\boldsymbol{t_{21}(z_i)} = \frac{\rho(z_i)[E^+(z_i) - E^-(z_i)]}{1-\rho(z_i)^2} e^{+j\Omega} \quad (4)$$

$$\boldsymbol{t_{22}(z_i)} = \frac{-[\rho(z_i)^2 E^+(z_i) - E^-(z_i)]}{1-\rho(z_i)^2} \quad (5)$$

Where Ω is the residue corrugation phase at z_0 and

$$\boldsymbol{E^{\pm}(z_i)} = e^{j(\beta_0 \pm \gamma(z_i))(z_{i+1}-z_i)} \quad (6)$$

β_0 And γ are, respectively, the propagation constant and the complex propagation constant given by:

$$\boldsymbol{\beta_0} = \frac{\pi}{\Lambda} \quad (7)$$

$$\boldsymbol{\gamma(z_i)} = \sqrt{(\alpha(z_i) - j\delta(z_i))^2 + \kappa(z_i)^2} \quad (8)$$

With α and δ are, respectively, the gain and detuning for the propagation mode inside the laser structure and κ the coupling coefficient. ρ Can be written as:

$$\boldsymbol{\rho(z_i)} = \frac{j\kappa(z_i)}{\alpha(z_i) - j\delta(z_i) + \gamma(z_i)} \quad (9)$$

For DFB laser structure having a fixed cavity length, one must determine both the amplitude gain coefficient α and the detuning coefficient δ for the section i in order that each matrix element $t_{jk}(j,k = 1,2)$ as shown in eqn (2)-(3)-(4) and (5) can be determined. For the first-order Bragg diffraction, the mode detuning and the gain can be expressed, respectively, for an arbitrary section i as [1]:

$$\boldsymbol{\delta(z_i)} = \frac{2\pi}{\lambda} \boldsymbol{n(z_i)} - \frac{2\pi n_g}{\lambda \lambda_B}(\lambda - \lambda_B) - \frac{\pi}{\Lambda(z_i)} \quad (10)$$

And

$$\boldsymbol{\alpha(z_i)} = \frac{\Gamma g(z_i) - \alpha_s}{2} \quad (11)$$

Where λ_B is the Bragg wavelength, λ is the lasing-mode wavelength, n is the refractive index, n_g is the group refractive index, Γ is the optical confinement factor, α_s is the total loss (includes the absorption in both the active and cladding layer as well as any scattering), and g is the material gain, given by:

$$\boldsymbol{g(z_i)} = A_0(N(z_i) - N^0) - A_1[\lambda - (\lambda_0 - A_2(N(z_i) - N_0))]^2 \quad (12)$$

In the above equation, N is the carrier concentration, A_0 is the differential gain, N_0 is the carrier concentration at transparency ($g = 0$), λ_0 is

Journal of Theoretical and Applied Information Technology
30th April 2012. Vol. 38 No.2

ISSN: 1992-8645 www.jatit.org E-ISSN: 1817-3195

the peak wavelength at transparency and A_1 and A_2 are parameters used in the parabolic model assumed for the material gain. Using the first-order approximation for the refractive index n, one obtains:

$$\mathbf{n(z_i) = n_0 + \Gamma \frac{\partial n}{\partial N} N(z_i)} \quad (13)$$

Where n_0 is the refractive index at zeros carrier injection and $\frac{\partial n}{\partial N}$ is the differential index.

The carrier concentration N and the stimulated photon density P are coupled together through the steady-state carrier rate equation $(\frac{\partial N}{\partial t} = 0)$ which is shown here as [1]:

$$\mathbf{\frac{I(z_i)}{qV} - \frac{N(z_i)}{\tau} - BN(z_i)^2 - CN(z_i)^3 - \frac{c_g g(z_i) P(z_i)}{1+\varepsilon P(z_i)} = 0} \quad (14)$$

Where I is the injection current, q is the modulus of the electron charge, V is the volume of the active layer, τ is the carrier life time, B is the radiative spontaneous emission coefficient, C is the Auger recombination coefficient, ε is a non-linear coefficient to take into account saturation effects and $c_g = c/n_g$ is the group velocity, with c being the free space velocity.

In index-coupled DFB laser cavity, the local photon density $P(z_i)$ inside the cavity can be expressed as [10]:

$$\boldsymbol{P(z_i) = \frac{2\varepsilon_0\, n(z_i) n_g \lambda}{hc} C_0^2 [|R(z_i)|^2 + |S(z_i)|^2]} \quad (15)$$

Where ε_0 is the free space permittivity, h is the Planck's constant and c_0 a dimensionless coefficient that allows the determination of the total electric field at the above-threshold regime, taking into account that the normalization

$$\mathbf{|R(0)|^2 + |S(0)|^2 = 1} \quad (16)$$

In this paper, the numerical procedure for the above-threshold calculations follows closely the method developed in [1]- [5]- [12].

In the above-threshold regime, P is high enough to induce important non-uniformities in N and n. Despite the SHB effect can be minimized by adequate design. In the proposed quarter-wavelength-shift distributed feedback diode laser structure it is supposed that, the coupling coefficient, κ, in the waveguide along the laser cavity changes continuously as follows:

$$\boldsymbol{\kappa(z) = \kappa_o e^{-G\left[(z-\frac{L}{2})/L\right]^2}} \quad (17)$$

Where L is the length of cavity, κ_o (average coupling coefficient), κ_o is introduced in order to allow a straightforward comparison between the standard QWS DFB laser structure ($G = 0$) and the GPCC QWS DFB laser ($G = 1$). The parameters definitions of the structures under analysis are summarized in table I, their coupling coefficient profiles are represented in Fig. 2.

TABLE I: SUMMARY PARAMETERS DEFINITIONS OF STRUCTURES:

G	Average normalized coupling coefficient $\kappa_o L$	Acronym
0	*2.50*	*Standard QWS-DFB*
1	*2.7098*	*GPCC QWS DFB*

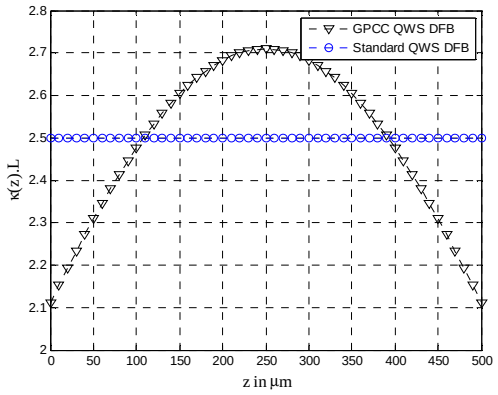

Fig. 2: Normalized coupling coefficient profiles used for the numerical simulations.

The material and structural parameters used in the analysis are summarized respectively in Table II and III.

TABLE II: SUMMARY OF MATERIAL PARAMETERS

Symbol	Parameters	Value
τ	Carrier lifetime	$4.10^{-9}s$
B	Bimolecular recombination	$10^{-16}\, m^3.s^{-1}$
C	Auger recombination	$3.10^{-41}\, m^6.s^{-}$
N_0	Transparency carrier density	$1.5.10^{24}\, m^{-3}$
ε	Non-linear gain coefficient	$1.5.10^{-23}\, m^3$
A_0	Differential gain	$2.7.10^{-20}\, m^6$
A_1	Gain curvature	$1.5.10^{19}\, m^{-3}$
A_2	Differential peak wavelength	$2.7.10^{-32}\, m^4$
α_l	Internal absorption	$4.10^3\, m^{-1}$
n_0	Refractive index at zero injection	3.41351524

Journal of Theoretical and Applied Information Technology
30th April 2012. Vol. 38 No.2

ISSN: 1992-8645 www.jatit.org E-ISSN: 1817-3195

$\frac{dn}{dN}$	Differential index	$-1.8.10^{-26}\ m^3$
n_g	Group index	3.7
c_g	Group velocity	$8.33.10^7\ m.s^-$

TABLE III: SUMMARY OF STRUCTURAL PARAMETERS

Symbol	Parameters	Value
L	Cavity length	$500\ \mu m$
D	Active layer thickness	$0.12\ \mu m$
W	Active layer width	$1.5\ \mu m$
V	Volume for active region	$90\ \mu m^3$
Λ	Grating period	$227.039\ nm$
λ_B	Bragg wavelength	$1.55\ \mu m$
Γ	Optical confinement factor	0.35
φ	Phase shift	90^0
Ω	Residue corrugation phase at left facet	0^0

3. NUMERICAL RESULTS AND DISCUSSION

The above-threshold model based on the transfer matrix is applicable to various types of distributed feedback laser structures. In this section, results obtained from standard QWS DFB and GPCC QWS DFB LDs, are presented.

The lasing characteristics and the distributed of the spatially dependent parameters like photon density, carrier concentration, refractive index and the normalized field intensity will be shown.

To maintain the single mode oscillation and to reduce the effects of spatial hole burning, DFB LD's showing a large normalized gain margin ($\Delta\alpha L$) between the lasing mode and the most probable side, and also a uniform internal field distribution are preferred. For a DFB LD having a cavity length of $500\ \mu m$, the criterion for the single longitudinal mode operation is that $\Delta\alpha L > 0.25$ [1]- [13]- [14]. Similarly, the internal field distribution of the laser should be fairly uniform in order that the spatial hole burning effect is suppressed. Flatness (F) value of less than 0.05 is assumed where F is given as [13]:

$$\mathbf{F} = \frac{1}{L}\int_0^L (I(z) - \bar{I})^2 dz \qquad (18)$$

Where $I(z)$ is the normalized electric field intensity at an arbitrary position, z, given by:

$$I(z) = \frac{|R(z)|^2 + |S(z)|^2}{|R(0)|^2 + |S(0)|^2} \qquad (19)$$

And $\bar{I}$ is its average value along the cavity.

The QWS DFB LD with uniform coupling coefficient has been used for some time because of its ease of fabrication, and because Bragg oscillation can be achieved readily with a single 90^0 phase shift [10]. From the threshold analysis, this DFB laser structure is characterized by a non-uniform field intensity which is vulnerable to the spatial hole burning effect. Experimental results [17] have demonstrated that the gain margin deteriorates quickly when the biasing current increases. For a strongly coupled device (i.e. $\kappa L \geq 1.75$), the side mode on the shorter wavelength side (+1 mode) become dominant. For a $300\ \mu m$ length cavity, two-mode operation at an output power of around $7.5\ mW$ was observed at a biasing current of $2.25 I_{th}$ [1].

The spatial hole burning effect alters the lasing characteristics of the QWS DFB LD by changing the refractive index along the cavity. Under a uniform current injection, the light intensity inside the laser structure increases with biasing current. For strongly coupled laser devices, most light concentrate at the centre of the cavity. The carrier density at the centre is reduced remarkably as a result of stimulated recombination. Such a depleted carrier concentration induces an escalation of nearby injected carriers and consequently a spatially varying refractive index results.

Using the TMM-based model, the above-threshold characteristics of the standard QSW DFB ,and GPCC QWS DFB are to be verified and compared, a $500\ \mu m$ long lasers cavity with a strongly coupled ($\kappa L = 2.5$) are assumed and a phase shift of 90^0 are located at the centre of the cavity.

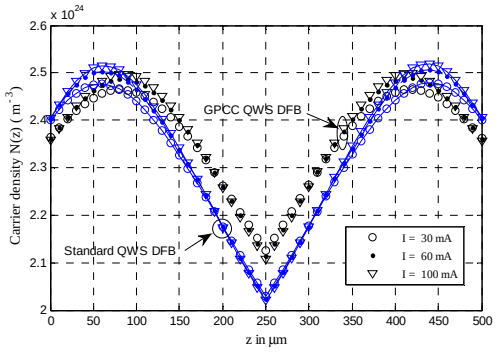

Fig. 3: Longitudinal distribution of carrier concentrations in Standard QWS DFB (The solid line) and in GPCC QWS DFB (no line) for different biasing currents.

In the Fig. 3, the carrier concentration profiles are shown with different injection currents. The

Journal of Theoretical and Applied Information Technology
30th April 2012. Vol. 38 No.2

ISSN: 1992-8645 www.jatit.org E-ISSN: 1817-3195

dynamic range of the carrier concentration increase with biasing current, the depleted carrier concentration observed near the centre of the cavity arises severe spatial hole burning. In the GPCC QWS DFB Laser structure, the carrier density profile shown appears to be more uniform, an increase in the biasing current shows little change in spatially distributed carrier distribution.

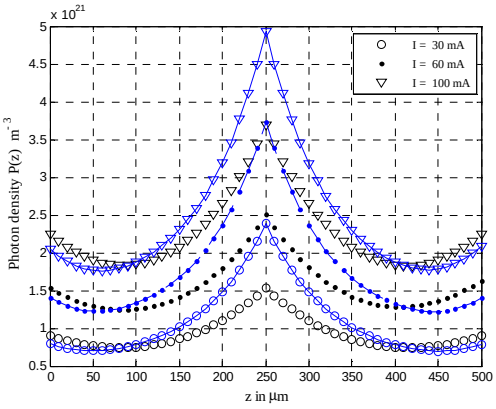

Fig. 4: Longitudinal distribution of photon density in Standard QWS DFB (The solid line) and in GPCC QWS DFB (no line) for different biasing currents.

Fig. 4 shows the spatial dependence of the photon density with biasing current changes for different structures under analysis. The photon distributions are fairly uniform when the biasing currents are close to its threshold values ($I < 30\,mA$); on the other hand, an overall increase in the photon density is observed with increasing biasing current. At the centre of the cavity, in particular, a peak value of the photon density is expected in such a strongly coupled device. An increase in the average photon density is also shown when the biasing current increase. However, it can be seen the use of a smaller coupling coefficient near the facet (GPCC QWS DFB Laser) has flattened out the photon distribution; the uniform photon distribution also reduces the difference between the central photon density and the escaping photon density at the facet, in particular at high biasing current ($I = 100\,mA$). Consequently, the GPCC QWS DFB Laser exhibits a large output optical power, which obviously constitutes the first advantage of this novel structure.

The variations of the spatially distributed refractive index are shown in Fig. 5, when the biasing current increases, the longitudinal span of the refractive index also increases. From Fig. 5, it can also be seen that the spatially distributed refractive index becomes saturated near the centre of the cavity at high biasing current. As the photon density increases with the biasing current, the photon density at the centre of the cavity becomes so high that the non-linear gain coefficient becomes dominant especially for the standard QWS DFB laser structure. Compared with the standard QWS laser structure, a more uniform distribution can be seen in the case of the GPCC QWS DFB structure, as shown in Fig. 5 the refractive index at the phase shift becomes saturated at high biasing current. In Fig. 6, the internal field intensity shows little change with increasing biasing current.

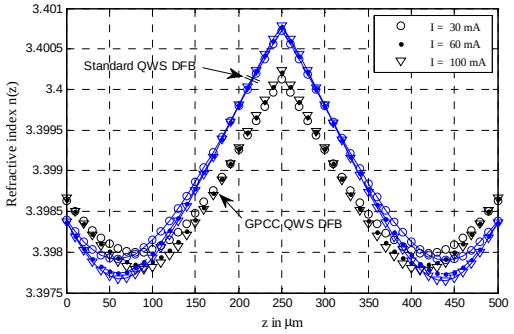

Fig. 5: Longitudinal distribution of refractive index in Standard QWS DFB (The solid line) and in GPCC QWS DFB (no line) for different biasing currents.

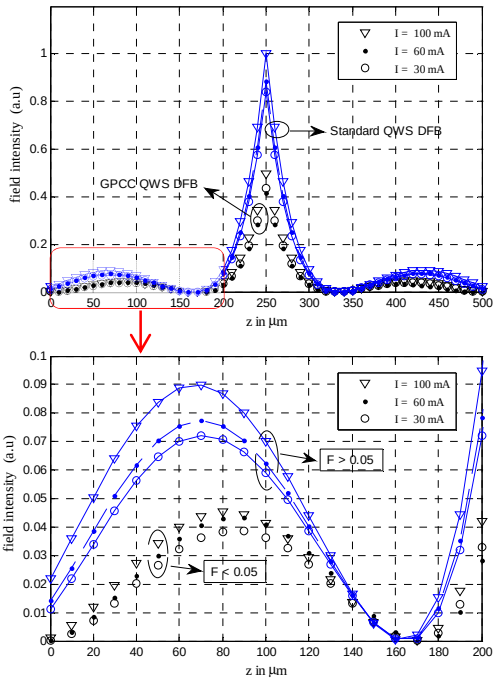

Fig. 6: Longitudinal distribution of the field intensity in Standard QWS DFB (The solid line) and in GPCC QWS DFB (no line) for different biasing currents.

Journal of Theoretical and Applied Information Technology
30th April 2012. Vol. 38 No.2

ISSN: 1992-8645 www.jatit.org E-ISSN: 1817-3195

From the emitting photon density at the facet, the output optical power can be evaluated. Fig. 7 summaries results obtained for the standard QWS DFB and GPCC QWS DFB LDs with the biasing current as parameter. Compared with the standard QWS DFB, it seems that the use of a smaller coupling coefficient near the facet has increased the overall cavity loss. The figure also shows that the GPCC QWS DFB laser structure has à relatively smaller value of threshold current (I_{th} = 19.75 mA) and a relatively larger output power under the same biasing current.

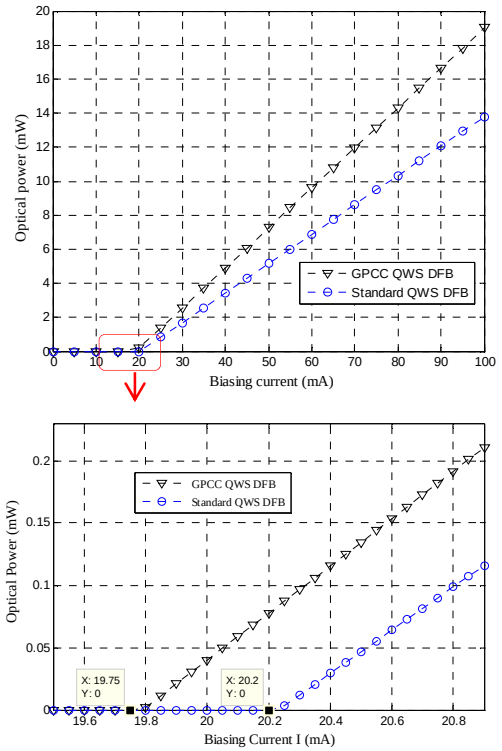

Fig. 7: Emitted optical power of standard QWS DFB and GPCC QWS DFB for different biasing currents

Semiconductor lasers having stable single longitudinal outputs are indispensable in coherent optical communication systems. With a built-in wavelength selective corrugation, a DFB laser diode has a single longitudinal output. Other oscillation modes failing to reach the threshold condition become the non-lasing side modes (SM). As the biasing current increases, the spatial hole burning effect becomes significant and mode competition between the lasing mode and the most probable non-lasing side mode may occur. Mode competition has been observed for a standard QSW DFB laser [17], which resulted in multiple mode oscillation as the biasing current increased.

Single-mode stability implies the suppression of non-lasing side modes. There are two possible ways to demonstrate single-mode stability in DFB LDs. The first approach involves the evolution of the normalized gain margin (ΔαL) between the lasing mode and the probable non-lasing side mode. The single-mode stability is said to be threatened if the normalized gain margin, (ΔαL) drops below 0.25. An alternative method to check the stability of the device involves the measurement of the spectral characteristics. With the help of an optical spectrum analyser, the measured intensity difference between the lasing mode and the side modes will give single-mode stability. The second approach is often used to measure the single-stability of the DFB LDs. In this paper we will concentrate on the first approach which leads to the evolution of the above-threshold gain margin.

From the numerical method discussed in the previous section, oscillation characteristics of the lasing mode were obtained at a fixed biasing current. By dividing the DFB laser into a large number of smaller sections, longitudinal distributions like the carrier and photon densities were determined. Since the laser cavity is now dominated by the lasing mode, the characteristics of other non-lasing side modes should be derived from the lasing mode. In order to evaluate the characteristics of other non-lasing side modes, a numerical procedure similar to one discussed in reference [13] is adopted.

Fig. 8 (a) shows the spectral characteristics of the standard QWS DFB laser structure with the biasing current changes, for each oscillating mode shown in fig the circle and the rectangle correspond to the from I = 30 mA and at I = 100 mA, respectively, when the biasing current increases from the threshold value, an increase in the lasing mode amplitude gain and a corresponding reduction of gain margin between the lasing mode and the (+1) side mode can be seen such a phenomenon is well known to be induced by the spatial hole burning effect [2]. With a Gaussian profile of the coupling coefficient, the characteristics of the GPCC QWS DFB laser structures are shown in Fig. 8 (b), compared with the Standard QWS DFB structure, the GPCC QWS DFB shows a smaller shift in mode characteristics. This may be clearer when the variation of the normalized amplitude gain margin is shown as a function of injection current. From Fig. 9 where the normalized amplitude gain margin change is shown, the injection current alters the oscillating mode in a different way, it can be observed that the normalized gain margin (ΔαL) between the lasing mode and the most probable

Journal of Theoretical and Applied Information Technology
30th April 2012. Vol. 38 No.2

ISSN: 1992-8645 www.jatit.org E-ISSN: 1817-3195

side mode (+1) shows little change, the lasing mode shown has a milder shift with increasing biasing current. On combining results from Fig. 8 and Fig. 9, it appears that the GPCC QWS DFB laser structure is not seriously affected by the spatial hole burning effect. No severe reduction of gain margin and a fairly mild in detuning (ΔδL) coefficient are observed.

a-

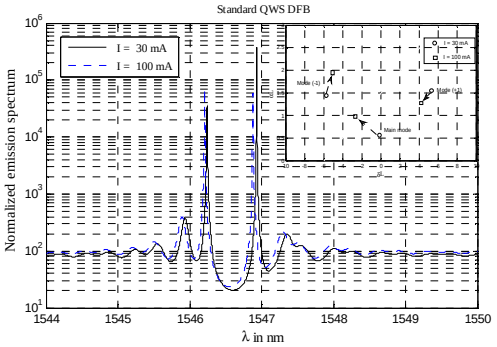

b-

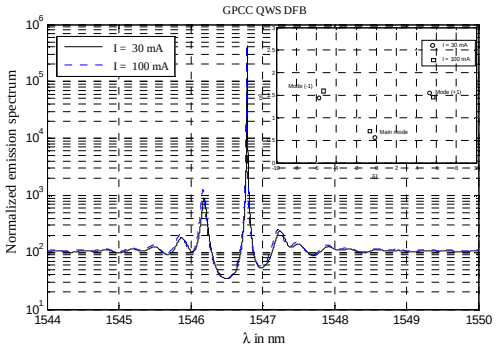

Fig. 8: The Normalized emission spectrum and the lasing characteristics of (a) the standard QWS DFB (b) GPCC QWS DFB

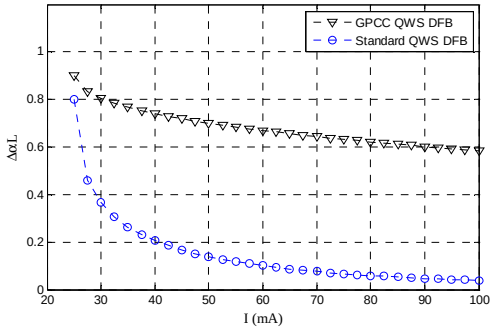

Fig. 9: The variation of gain margin with respect to changes in the injection current for different structures.

The fig. 8-a also shows the spectral characteristics (emission spectrum) of the standard QWS DFB laser structure with the biasing current changes. Along a fixed biasing current, distinct peaks can be seen along the spectrum which corresponds to different oscillating modes. The lasing mode shown near 1546.90 nm becomes the lasing after the threshold condition is reached, when the biasing current increases (100 mA) it can be seen that all peak wavelengths shift towards the shorter wavelength, the so-called 'blue shift' in wavelength follows the change of material gain with carrier concentration which has been demonstrated experimentally using a standard QSW DFB LD [17], apart from that, a reduction of the spectral amplitude difference is also shown between the lasing mode and the (+1) mode which is located at shorter wavelength side. At a biasing current of 100 mA, the side mode suppression ratio (SMSR) is reduced to less than 25 dB. At such an SMSR value. The stability of the single mode oscillation is weakened and the presence of the +1 mode becomes significant in the case of a QWS DFB LD.

As with the standard QWS DFB laser structure, distinct peaks which correspond to different oscillating modes are observed along the spectrum (Fig. 8-b), when the biasing current increases, the spectral amplitude of the dominant lasing mode found near 1546.78 nm shows no sign of reduction and remains at a high value near 10^6. Compared with the standard QWS DFB structure, the GPCC QWS DFB laser structure shows no server mode competition and an SMSR at least 25 dB is maintained throughout the range of biasing current.

4. CONCLUSION

In this paper, the above-threshold of the standard and GPCC quarter-wavelength-shift distributed feedback diode lasers structures were investigated using the transfer matrix method. To take into account any changes in the biasing current, the carrier rate equation was included, in the analysis multi-carrier recombination and a parabolic gain model have been assumed, to include any gain saturation effects, a non-linear gain coefficient was introduced into analysis. The TMM-based above-threshold laser model was applied to standard QWS DFB and the proposed GPCC QWS DFB, the standard QWS DFB, which is characterized by its non-uniform field distribution, was shown to have a large dynamic change of the spatially distributed refractive index. Along the carrier concentration profile, a dip was shown at the centre of the cavity

ISSN: 1992-8645 www.jatit.org E-ISSN: 1817-3195

where the largest stimulated photon density is found.

The field distribution in the QWS DFB LD can be improved by introducing the continuously distributed coupling coefficient. In the analysis, a PGCC QWS DFB laser structure was used, as compared with the QWS structure; uniform distributions were observed in the carrier density, photon density and refractive index profiles.

From the lasing mode distributions of the carrier density, photon density, refractive index and field intensity, characteristics like the single-mode stability and the emission spectrum have been investigated throughout the analysis. At fixed biasing current, it is shown that standard QWS structure showing the largest threshold current has the smallest output optical power. On the other hand, this structure has a very poor single-mode stability and the (+1) non-lasing side mode becomes influential when the biasing current increases. The introduction of coupling coefficient with a Gaussian profile has improved the single-mode stability such the SMSR remains at high value.

REFRENCES:

[1] H. Ghafouri-shiraz, Distributed feedback laser diodes and optical tunable filters, Birminghman, UK: WILEY, 2003.

[2] A. Zatni and J. Le Bihan, "Analysis of FM and AM responses of a tunable three-electrode DBR laser diode," *IEEE Journal of Quantum Electronics*, vol. 31, pp. 1009-1014, 1995.

[3] T. Fessant, "multisection distributed feedback lasers with a phase-adjustment region and a nonuniform coupling coefficient for high immunity against spatial hole burning," *optic communications*, vol. 148, pp. 171-179, 1998.

[4] S. N Mohammad, "Axial distribution of coupling coefficient of distributed feedback laser diode," *optics & laser technology* , vol. 39, pp. 290-293, 2007.

[5] José A.P. Morgado, Carlos A.F Fernandes, Jose B. M. Bovida "Novel DFB laser structure suitable for stable single longitudinal mode operation," *Optics & Laser Technology*, vol. 42, pp. 975-984, 2010.

[6] A.Zatni, "Study of the short pulse generation of the three quarter wave shift DFB laser (3QWS-DFB)," *ANNALS OF TELECOMMUNICATIONS*, vol. 60, pp. 698-718, 2005.

[7] Jing.-Yi. Wang and Michael Cada, "analysis and optimum desing of distributed feedback lasers using coupled-power theory," *IEEE journal of quantum electronics*, vol. 36, pp. 52-58, 2000.

[8] A.Moumen, A. Zatni "Above-threshold characteristics of DFB laser diode: A TMM Approach," in *4th International Workshop on Smart Materials and Structures & International Meeting on Materials for Electronic Applications IMMEA-2011*, Agadir, 2011.

[9] T. Fessant, "Threshold and above-threshold analysis of corrugation-pitch-modulated DFB lasers with inhomogeneous coupling coefficient," *IEE Proc., Optoelectron*, vol. 144, pp. 365-376, 1997.

[10] Whiteaway,J.E.A. Thompson, G.H.B. Collar, A.J. Armistead, C.J., "the design and assessment of $\pi/4$ phase shift DFB laser structures," *IEEE J. Quantum Electron*, vol. 25, pp. 1261-1279, 1989.

[11] F.Shahshahani,V.Ahmadim K. Mirabbaszadeh "concave tapered grating design of DFB laser at high power operation for reduced spatial hole-burning effect," *materials science and engineering* , vol. B96, pp. 1-7, 2002.

[12] S. K. B. Lo,H. Ghafouri-shiraz , "A method to dermine the above-threshold stability of distributed feedback semiconductor laser diodes," *journal of lightwave technology*, vol. 13, pp. 563-567, 1995.

[13] S. K. B. Lo,H. Ghafouri-shiraz, "Spectral characteristics of distributed feedback laser diodes with distributed coupling coefficient," *IEEE/OSA Journal of Lightwave Technology*, vol. 13, pp. 200-212, 1995.

[14] Carlos. A. F. Fernandes, Jose B. M, Bovida "optimisation of an asymmetric three phase-shift distributed feedback semiconductor laser structure concerning the above-threshold stability," *The European Physical Journal Applied Physics*, vol. 49, pp. 1-9, 2010.

[15] A. Zatni, J. Le Bihan, A. Charaia and D. Khatib, "FM and AM responses of a three-electrode DBR laser diode," *The 1st International Conference on Information & Communication Technologies: from Theory to Applications - ICTTA'04*, pp. 167-168, 2004.

[16] A.Moumen, A. Zatni "above-threshold analysis of distributed feedback semiconductor lasers strucures using the transfer matrix modelling," in *international symposium on*

ISSN: 1992-8645 www.jatit.org E-ISSN: 1817-3195

advanced materials for optics micro-electronics and nanoelectronics AMOMEN'2011, kénitra, 2011.

[17] Soda, H.; Kotaki, Y.; Sudo, H.; Ishikawa, H.; Yamakoshi, S.; Imai, H.; "stabilty in single longitudianl mode opeartion in GaInAsP/InP phase-adjusted DFB lasers," *IEEE J. quantum electron*, vol. 23, pp. 804-814, 1987.

[18] A. Zatni, D. Khatib, M. Bour, J. Le Bihan "Analysis of the spectral stability of the three phase shift DFB laser (3PS-DFB)," *Annals of Telecommunications*, vol. 59, pp. 1031-1044, 2004.

[19] C. A. F. Fernandes, "Stability in single longitudinal mode operation in DFB laser structures," in *IEEE MELECON*, Dubrovnik, croatia, 2004.